Electronic Supplementary Material

Copper-hydride nanoclusters with enhanced stability by N-heterocyclic carbenes

Hui Shen[1], Lingzheng Wang[1], Omar López-Estrada[2], Chengyi Hu[1], Qingyuan Wu[1], Dongxu Cao[1], Sami Malola[2], Boon K. Teo[1], Hannu Häkkinen[2] (✉), and Nanfeng Zheng[1] (✉)

[1] *State Key Laboratory for Physical Chemistry of Solid Surfaces, Collaborative Innovation Center of Chemistry for Energy Materials, National & Local Joint Engineering Research Center of Preparation Technology of Nanomaterials, College of Chemistry and Chemical Engineering, Xiamen University, Xiamen 361005, China*

[2] *Departments of Physics and Chemistry, Nanoscience Center, University of Jyväskylä, FI-40014 Jyväskylä, Finland*

Supporting information to https://doi.org/10.1007/s12274-021-3389-9

Experimental Details

Reagents: Cupric(II) acetylacetonate ($Cu(acac)_2$, 99%), 1,4-dibromobutane (98%, $C_4H_{10}Br_2$), benzimidazole ($C_7H_6N_2$, 99%), benzyl chloride (BnCl, 98%), iodine (I_2, 99%), tert-butyl hydroperoxide (TBHP, 98%), potassium t-butoxide (KO^tBu, 99%), tetrakis(acetonitrile)copper(I) tetrafluoroborate ($[Cu(CH_3CN)_4]BF_4$, 99%) and 4-fluorothiophenol (4-F-C_6H_5SH) are purchased from Innochem (Beijing, China). Sodium borohydride ($NaBH_4$, 98%), dichloromethane (CH_2Cl_2, A.R.), methanol (CH_3OH, A.R.), hexane (C_6H_{14}, A.R.) and ether ($C_4H_{10}O$, A.R.) were purchased from Sinopharm Chemical Reagent Co. Ltd (Shanghai, China). All reagents were used as received without further purification. Water used in all experiments was ultrapure. All other solvents were purified and degassed by standard procedures.

Synthesis of 1-benzyl-1H-benzimidazole (1a).

Compound 1-benzyl-1H-benzimidazole (**1a**) was prepared according to the literature.[1] The benzotriazole (0.50 mmol), toluene (2.0 mmol), I_2 (0.050 mmol), and TBHP (2 equiv) were taken in a round-bottom flask equipped with a stirrer. The resulting mixture was stirred for 10 h at 100 °C. After cooling to room temperature, to the reaction mixture was added H_2O (2 mL) and extracted with ester (3 × 10 mL). The combined organic phases were washed with brine (2 × 5 mL), dried over anhydrous $MgSO_4$, and concentrated in vacuo. The residue was subjected to flash column chromatography with hexane-EtOAc (10:1) as eluent to obtain the desired **1a** a light yellow solid. Yield: 65%.

Synthesis of 1,4-Bis(1-benzyl-1H-benzimidazol-1-ium-3-yl) butane Dibromide (1b).

Compound 1,4-Bis(1-benzyl-1H-benzimidazol-1-ium-3-yl) butane dibromide (**1b**) was prepared according to the literature.[2] To a suspension of N-benzylbenzimidazole (**1a**) (4.08 g, 20 mmol) in acetonitrile (30 mL) was added 1,4-dibromobutane (1.31 g, 7 mmol), and the mixture was refluxed for 72 h. The precipitate formed was filtered, washed with a small amount of acetonitrile, and dried in air. Recrystallization from boiling methanol with subsequent vacuum drying afforded the title compound as a white powder. Yield: 59%.

Synthesis of 1,4-Bis(1-benzyl-1H-benzimidazol-1-ium-3-yl) butane dicopper dbromide (1c).

Compound 1,4-Bis(1-benzyl-1H-benzimidazol-1-ium-3-yl) butane dicopper dbro-mide (**1c**) was prepared according to the literature.[3] A mixture of 1,4-Bis(1-benzyl-1H-benzimidazol-1-ium-3-yl) butane di-bromide (**1b**) (0.95 g, 1.5 mmol) and copper(I) chloride (0.3 g, 3.0 mmol) was dissolved in MeCN (15 ml), Et_3N (0.5 ml, 3.6 mmol) was added, and the mixture was boiled for 2 h. Then more Et_3N (0.5 ml, 3.6 mmol) was added, and refluxing was continued for 30 min. The reaction product was precipitated with water, filtered off, washed with a 1:3 2-PrOH-petroleum ether mixture for several times. Recrystallization of the residue from MeCN affords the product as yellow powder. Yield: 52%.

Synthesis of $Cu_{31}(NHC)_3(RS)_{25}H_6$ ($Cu_{31}H_6$).

The synthesis of $Cu_{31}(NHC)_3(RS)_{25}H_6$ ($Cu_{31}H_6$) was conducted in one-pot. In a typical synthesis, 650 mg (1 mmol) freshly-prepared precursor **1c** was dissolved in 125 mL mixed solvents of dichloromethane and methanol under ultrasonication. After stirring the solution for 20 min, 200 μL 4-fluorothiophenol and 500 μL triethylamine were added. The mixture was stirred for further 10 min. Then 10 equivalent $NaBH_4$ in MeOH was added. After aging the reaction for further 3 h, the mixture was thoroughly washed with water. After that, the solution in organic phase was subjected to the diffusion of hexane at -4 °C. Orange plate crystals were obtained in the yield of 29.6% (based on Cu) after six weeks. $Cu_{31}(NHC)_3(RS)_{25}D_6$ ($Cu_{31}D_6$) was synthesized with the same process by using $NaBD_4$ instead of $NaBH_4$.

Synthesis of $Cu_{61}(S^tBu)_{26}S_6Cl_6H_{14}$ (Cu_{61}).

Cluster $Cu_{61}(S^tBu)_{26}S_6Cl_6H_{14}$ was prepared according to modified method in the literature.[4] 63 mg of the $[Cu(CH_3CN)_4]BF_4$ was first dissolved in 3 mL of acetonitrile. 36 μL of tert-butyl thiol was then added to the solution followed by additions of 0.2 mL triethylamine. The reaction mixture was stirred for 3 h. Subsequently, the solvent was removed and the residue was dissolved in 3 mL chloroform. Then, 25 mg of borane tert-butylamine complex in 1 mL chloroform was added. The color of the solution changed slowly from light yellow to light red over time and the solution was continued stirring for 4 h. Finally, 4 mL of ethanol was added to this solution. The final solution was kept under a dark environment at room temperature and dark red crystals of the cluster were obtained after a week.

Address correspondence to Nanfeng Zheng, nfzheng@xmu.edu.cn; Hannu Häkkinen, hannu.j.hakkinen@jyu.fi

Synthesis of $Cu_{25}H_{22}((p\text{-}FPh)_3P)_{12}$ (Cu_{25}).

Cluster $Cu_{25}H_{22}((p\text{-}FPh)_3P)_{12}$ was prepared according to the literature.[5] Cupric(II) acetylacetonate (180 mg) was dissolved in 10 mL CH_3OH and 40 mL CH_2Cl_2. After vigorously stirring for 30 min, 300 mg $(p\text{-}FPh)_3P$ was quickly added and the color of the reaction solution changed from ink blue to light blue. After that, ice-cold aqueous $NaBH_4$ was quickly added. The reaction was aged for 5 hours. Black crystals were crystallized from CH_2Cl_2/hexane with few drops of ethanol after about 2 days at -4 °C.

Characterizations.

UV/Vis spectra were collected by Shimadzu UV-2550 Spectrophotometer using a quartz cuvette of 1 mm path length. Mass spectra were recorded on Apex Ultra 7.0 T fourier transformation ion cyclotron resonance mass spectrometry in positive mode. ^1H and ^{13}C NMR spectra were recorded at room temperature on a Bruker AV-500 and Bruker AV-850 spectrometer with TMS and solvent residual signal as an internal reference. X-ray single-crystal analysis: The diffraction data of the single crystals nanocluster $Cu_{31}(NHC)_3(RS)_{25}H_6$ was collected on an Agilent Technologies SuperNova system X-ray single-crystal diffractometer using Cu Kα (λ= 1.54184 Å) at 100 K. The data were processed using CrysAlisPro.[6] The structure was solved and refined using Full-matrix least-squares based on F2 using ShelXT,[7] ShelXL[8] in Olex2,[9] and Shelxle.[10] The thermal elipsoids of the ORTEP diagram were done at 50% probability. Detailed crystal data and structure refinements for the three compounds are given in Table S1. CCDC 2050535 contains the supplementary crystallographic data for this paper. These data are provided free of charge by The Cambridge Crystallographic Data Centre.

DFT for the electronic structure and optical spectra.

The density functional theory calculations were performed using the code package GPAW with the PBE (Perdew- Burke-Ernzerhof) approximation for the exchange-correlation functional.[11-12] Structural relaxation was done in real-space grid with spacing of 0.2 Å, and with a unit cell including 6 Å of vacuum around the cluster in all directions. Structure optimization was started from the experimental coordinates (CIF) with a convergence criterion for residual force per atom of 0.05 eV/Å. The model cluster without hydrides was formed for comparison from the experimental hydride cluster by removing the hydrides and relaxing the system. After relaxation, electronic and optical properties were analysed using 0.25 Å grid spacing. Local atomic charges were calculated with Bader method.[13-14] The optical response was computed with the linear-response time-dependent density functional theory (LR-TDDFT) as implemented in GPAW.[15] The PBE functional was used in the transition coupling kernel of the Casida formalism. The symmetries of the electron states were determined by projecting the Kohn-Sham states into spherical harmonics functions centered at the center of mass of the cluster.[16] Molecular dynamics were run using Langevin thermostat with 0.2 Å grid spacing, 2 fs time step and target temperature of 300K. To enable the larger time step the masses of hydrides and hydrogen atoms were doubled. The total length of the runs was 4.3-4.5 ps which included the heating. Friction parameter for the thermostat was set to 0.01.

DFT for NMR calculations of hydrides.

The magnetic shielding tensors were computed in deMon2k[17] code employing the Auxiliary Density Functional Theory (ADFT) approach. The optimized structure of $Cu_{31}H_6$ was taken from the GPAW calculation as described above. Two computations were performed with the level of following two approximations. PBE/SDD/DZVP: The relativistic Stuttgart–Dresden (SDD) pseudopotential[18] (Cu is described by a valence of 19 electrons) along with the DZVP[19] basis set (P, C, N, F, S and H). PBE/DZVP–ALL: The all electron description for the Cu atoms is used, DZVP basis set (Cu, P, C, N, F, S and H). All the computations were performed in combination with the GEN-A2* auxiliary function set. Each 1H chemical shift was referenced to the ^1H TMS chemical shift computed in PBE/DZVP–ALL.

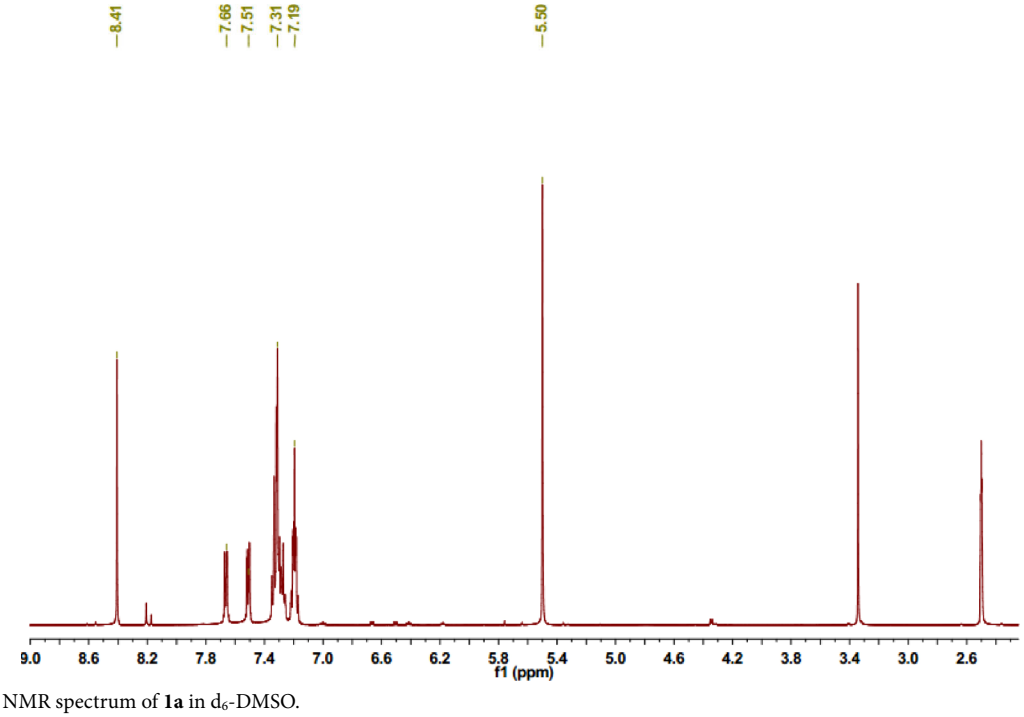

Figure S1 ^1H NMR spectrum of **1a** in d_6-DMSO.

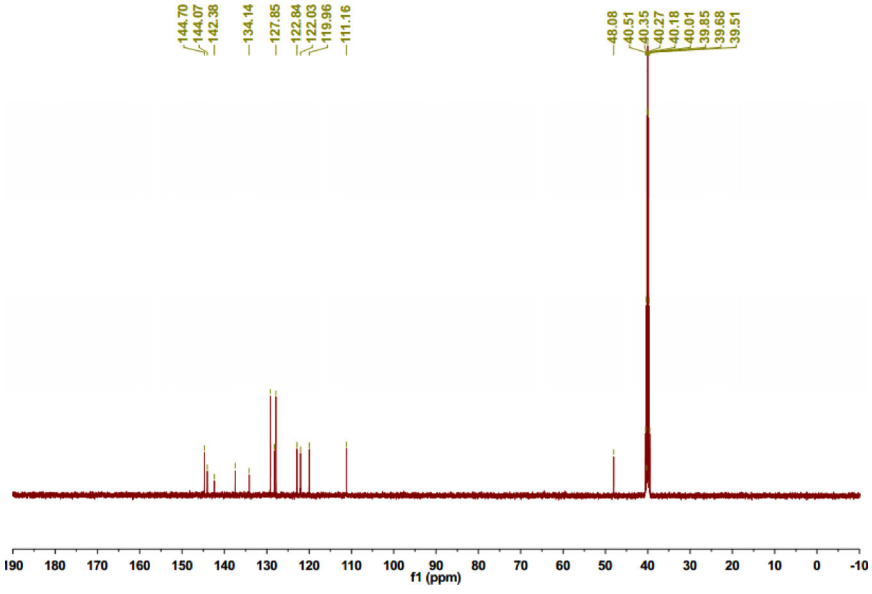

Figure S2 ^{13}C NMR spectrum of **1a** in d_6-DMSO.

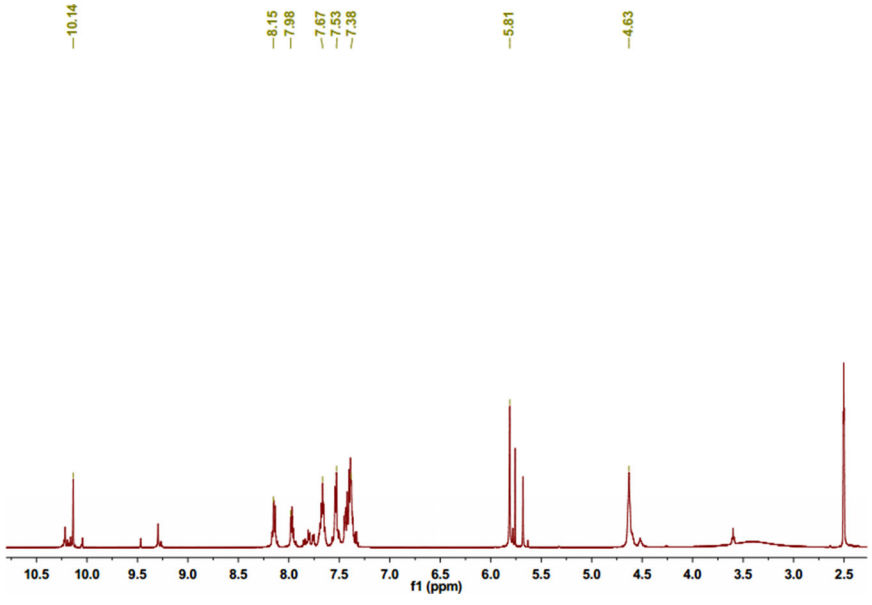

Figure S3 ^{1}H NMR spectrum of **1b** in d_6-DMSO.

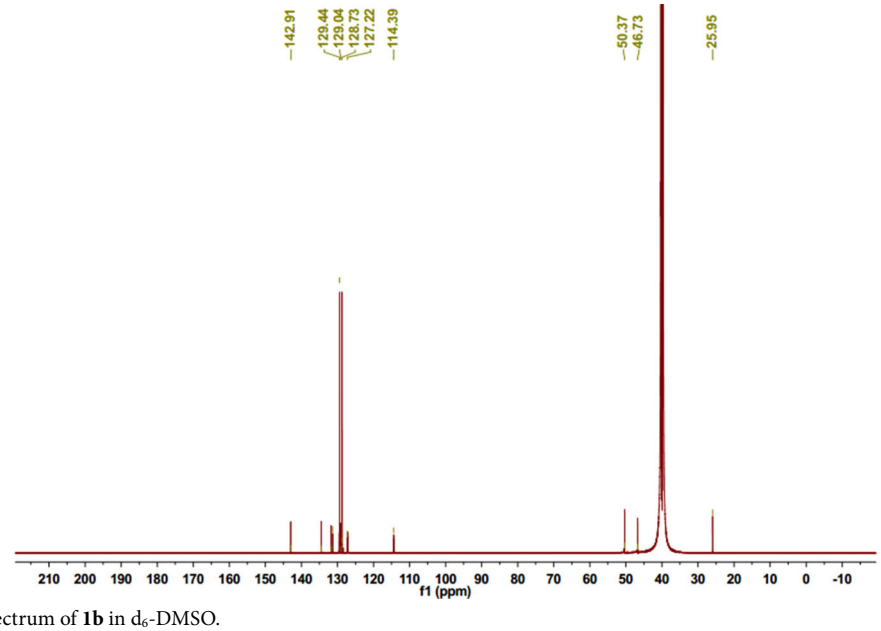

Figure S4 ^{13}C NMR spectrum of **1b** in d_6-DMSO.

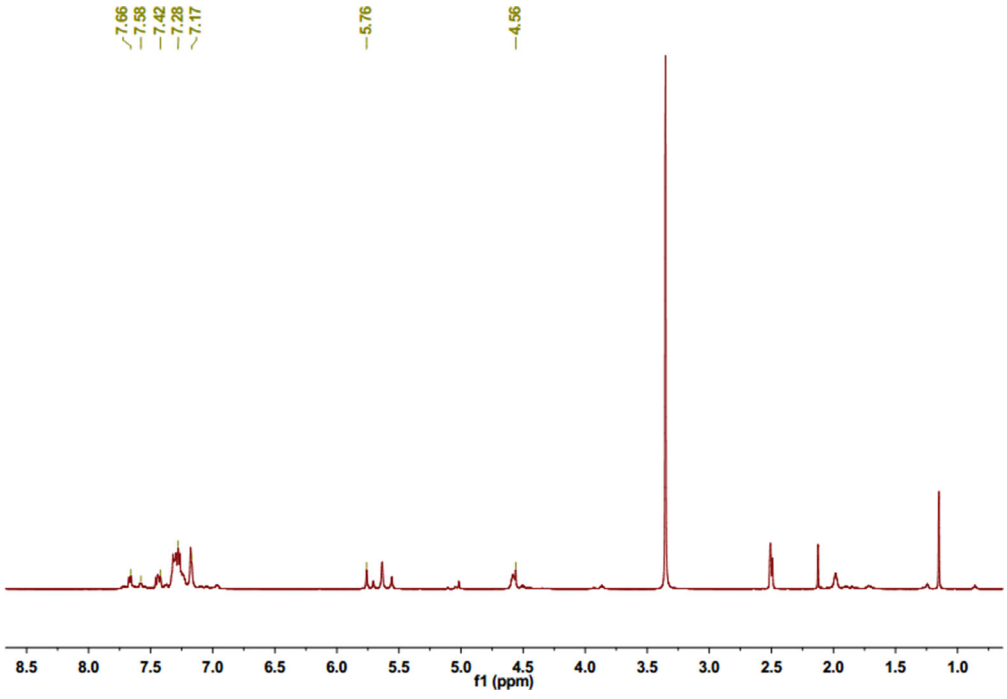

Figure S5 ^{1}H NMR spectrum of **1c** in d_6-DMSO.

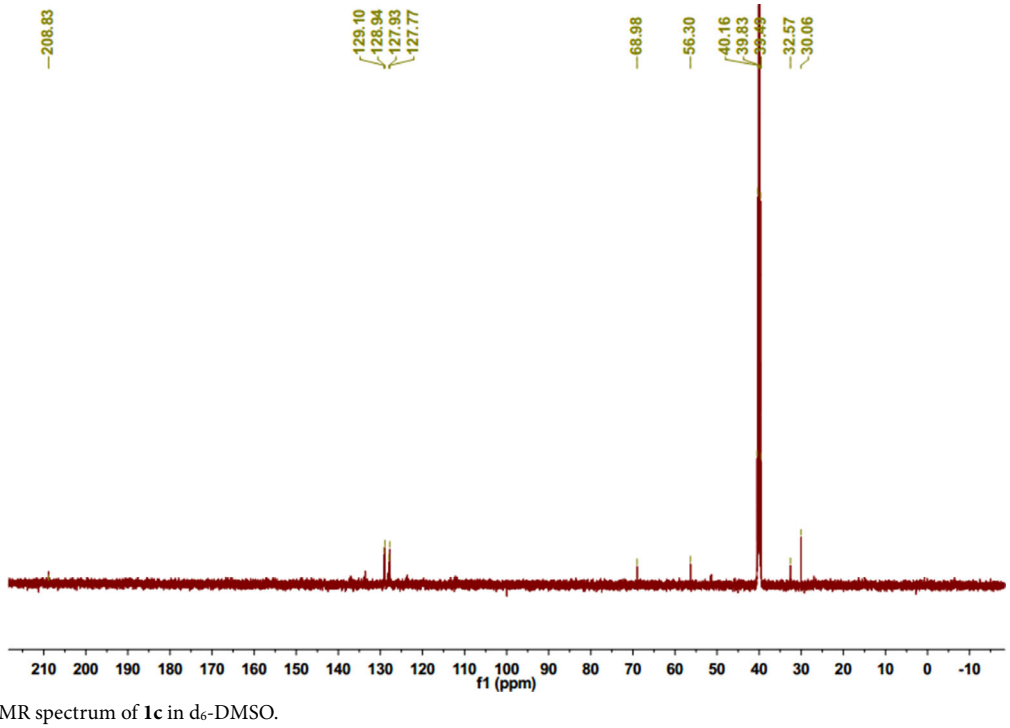

Figure S6 ^{13}C NMR spectrum of **1c** in d_6-DMSO.

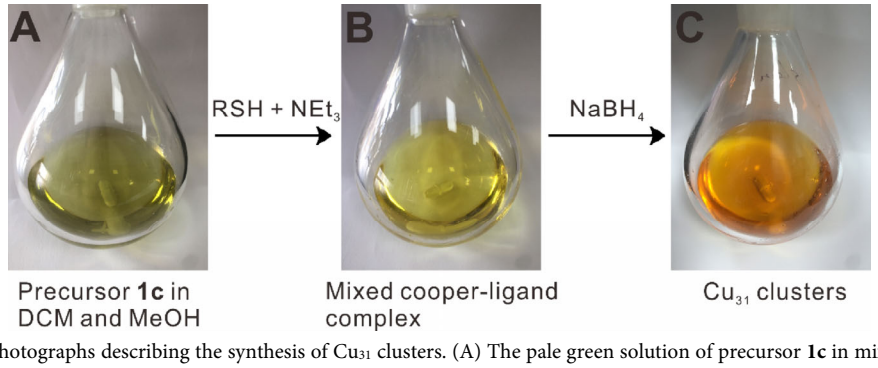

Figure S7 The digital photographs describing the synthesis of Cu_{31} clusters. (A) The pale green solution of precursor **1c** in mixed solvents of DCM and MeOH. (B) The solution turns into yellow after introducing RSH and NEt_3. (C) A orangish solution of Cu_{31} clusters were formed after reduction of metal-ligand complexes by $NaBH_4$.

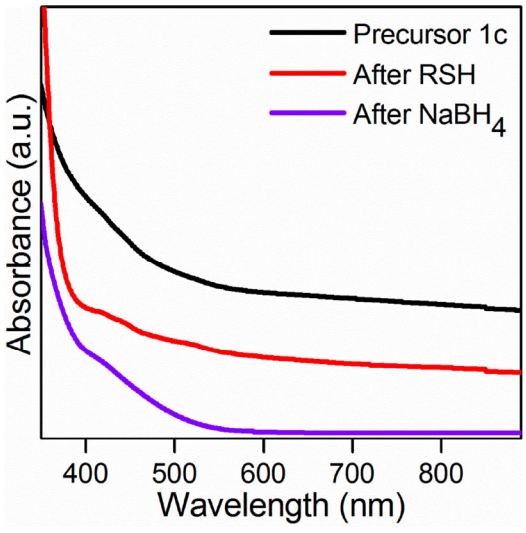

Figure S8 The UV/Vis absorption spectra of the solution recorded at different times during the synthesis of $Cu_{31}H_6$ cluster.

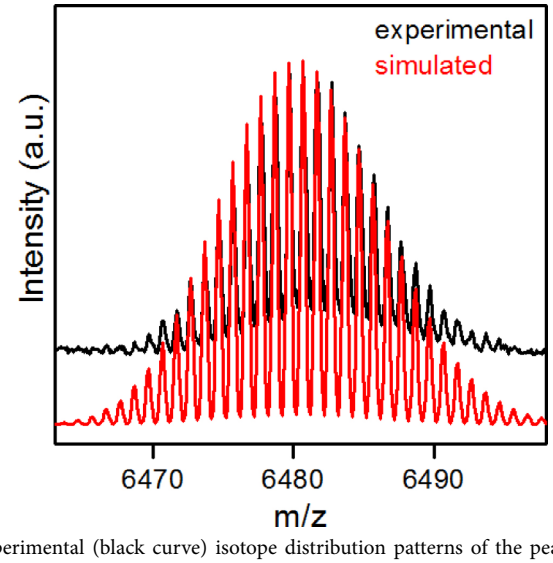

Figure S9 Simulated (red curve) and experimental (black curve) isotope distribution patterns of the peak marked as ϕ in Figure 1a. The simulated formula is $[Cu_{31}(NHC)_3(RS)_{24}H_6(CH_3CN)]^+$. CH_3CN was used as solvent for dissolving cluster sample in MS measurement.

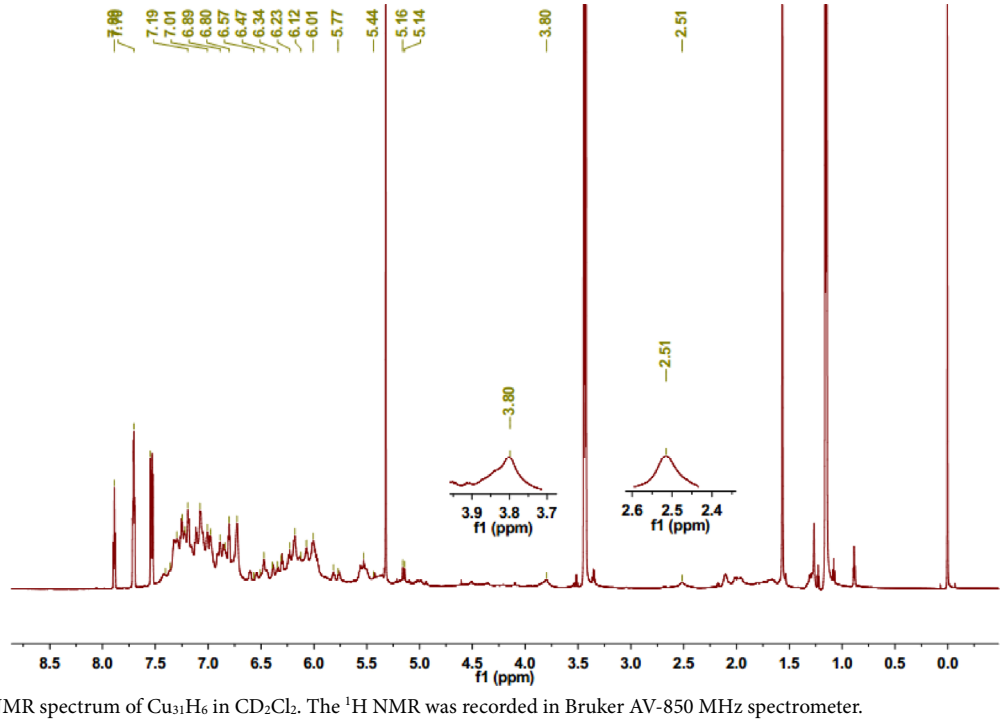

Figure S10 ^1H NMR spectrum of $Cu_{31}H_6$ in CD_2Cl_2. The ^1H NMR was recorded in Bruker AV-850 MHz spectrometer.

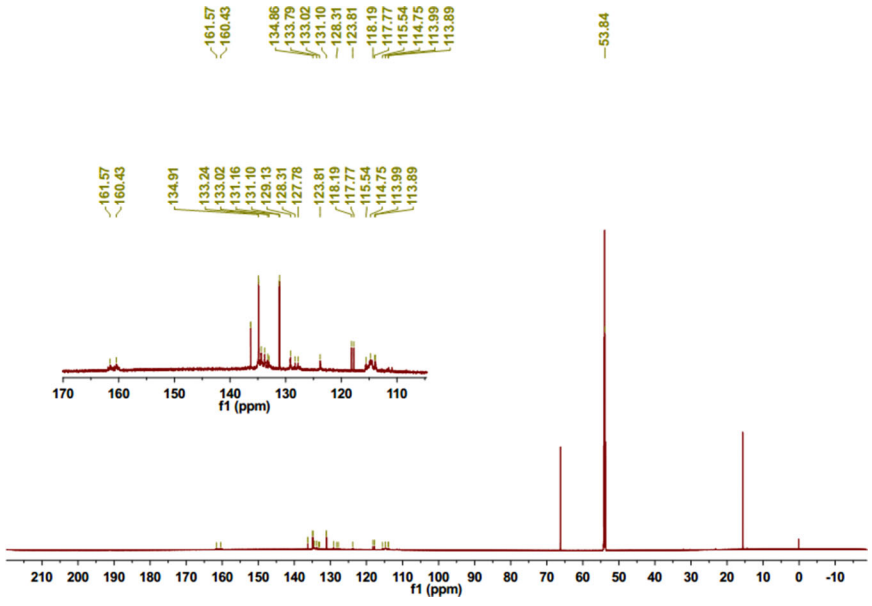

Figure S11 ^{13}C NMR spectrum of $Cu_{31}H_6$ in CD_2Cl_2. The ^{13}C NMR was recorded in Bruker AV-850 MHz spectrometer.

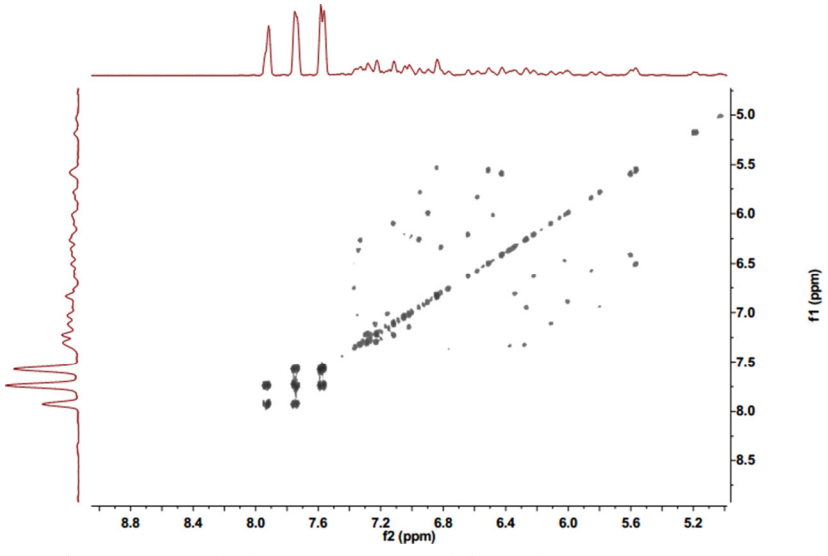

Figure S12 2D H-H COSY map of $Cu_{31}H_6$ in CD_2Cl_2. The spectrum was recorded in Bruker AV-850 MHz spectrometer. Only typical ligand regions are presented.

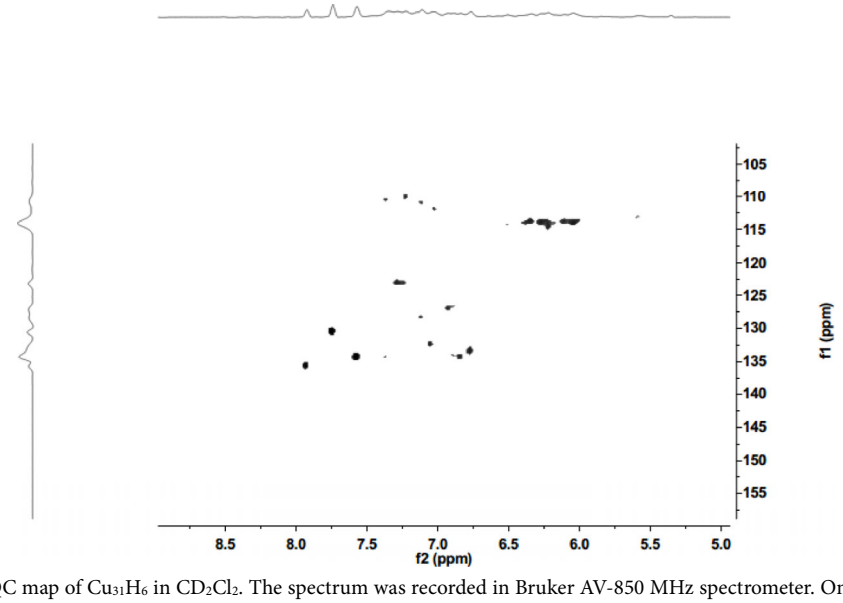

Figure S13 2D H-C HSQC map of $Cu_{31}H_6$ in CD_2Cl_2. The spectrum was recorded in Bruker AV-850 MHz spectrometer. Only typical ligand regions are presented.

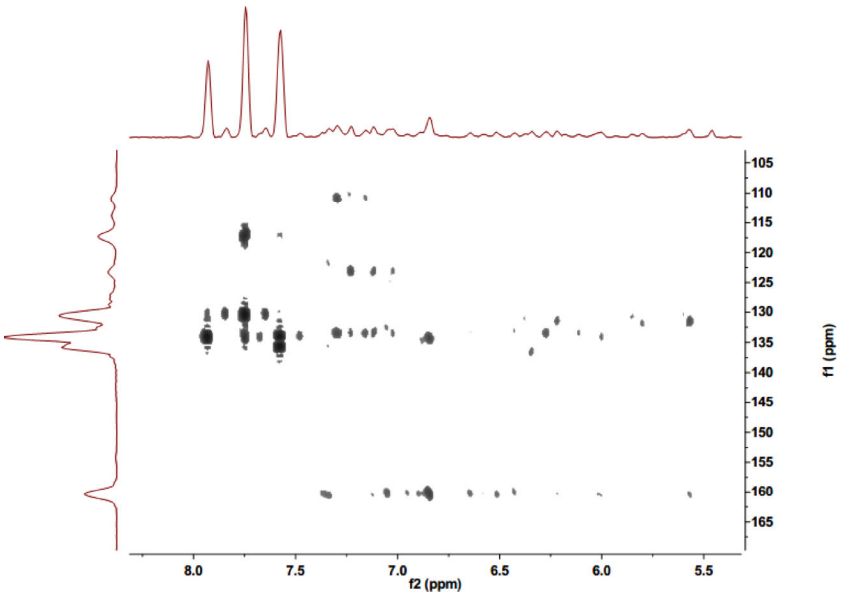

Figure S14 2D H-C HMBC map of $Cu_{31}H_6$ in CD_2Cl_2. The spectrum was recorded in Bruker AV-850 MHz spectrometer. Only typical ligand regions are presented.

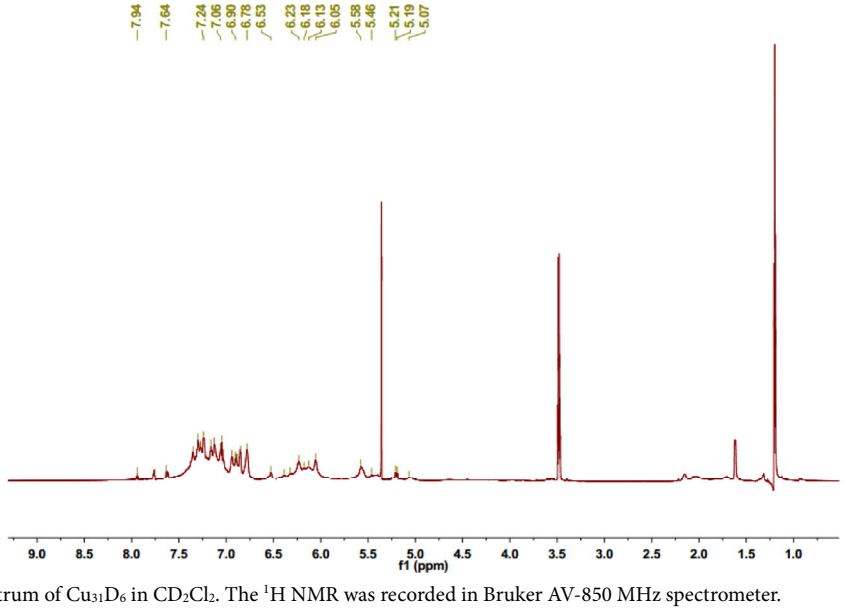

Figure S15 ^{1}H NMR spectrum of $Cu_{31}D_6$ in CD_2Cl_2. The ^{1}H NMR was recorded in Bruker AV-850 MHz spectrometer.

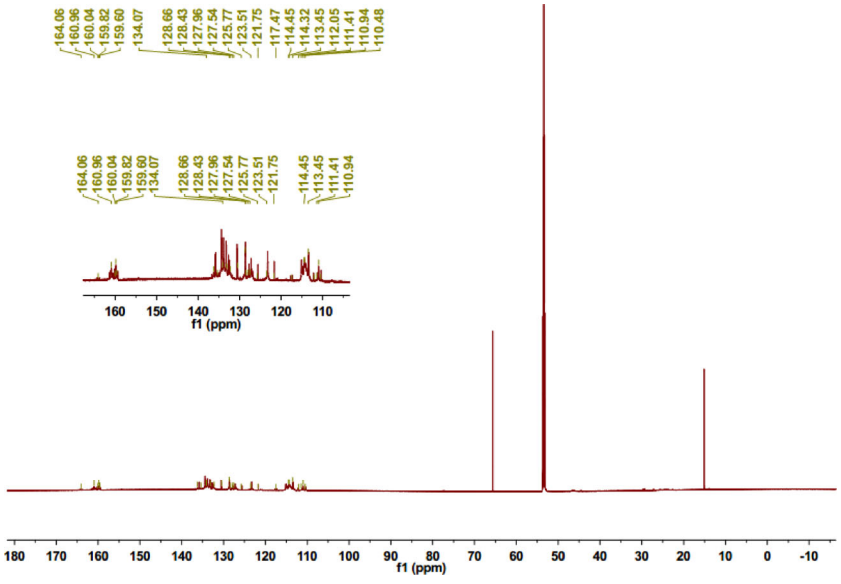

Figure S16 ^{13}C NMR spectrum of $Cu_{31}D_6$ in CD_2Cl_2. The ^{13}C NMR was recorded in Bruker AV-850 MHz spectrometer.

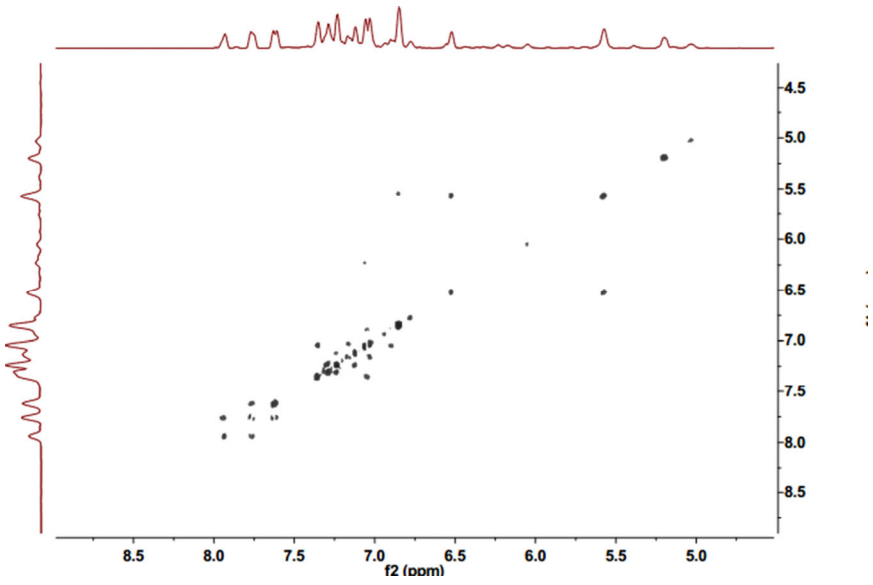

Figure S17 2D H-H COSY map of $Cu_{31}D_6$ in CD_2Cl_2. The spectrum was recorded in Bruker AV-850 MHz spectrometer. Only typical ligand regions are presented.

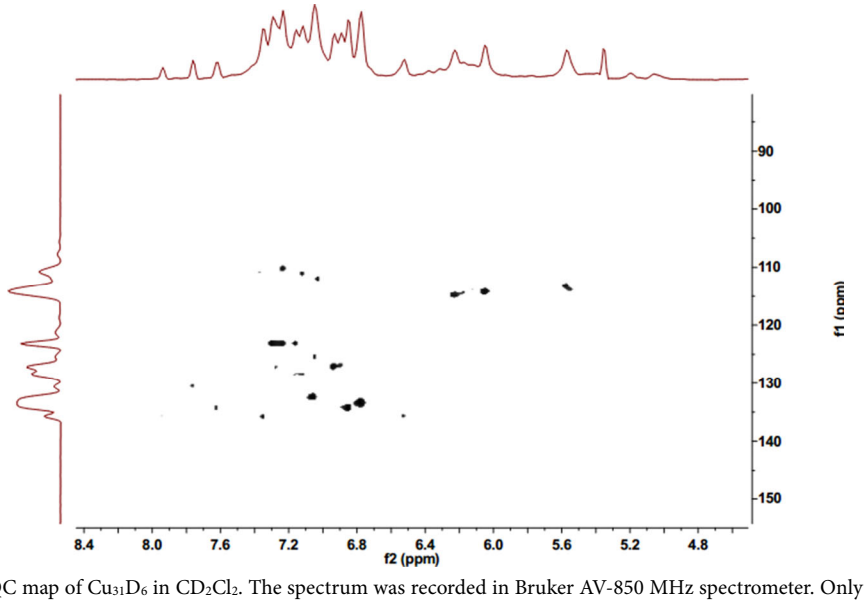

Figure S18 2D H-C HSQC map of $Cu_{31}D_6$ in CD_2Cl_2. The spectrum was recorded in Bruker AV-850 MHz spectrometer. Only typical ligand regions are presented.

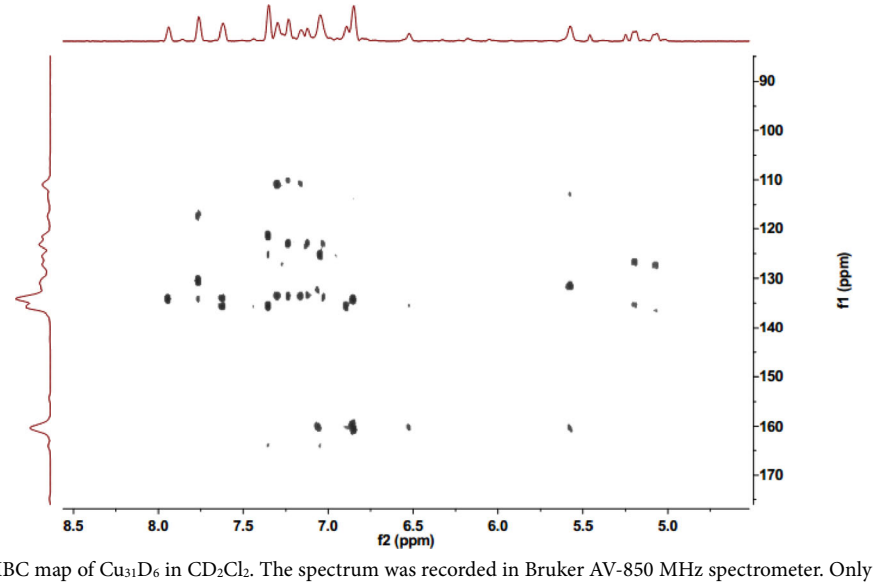

Figure S19 2D H-C HMBC map of $Cu_{31}D_6$ in CD_2Cl_2. The spectrum was recorded in Bruker AV-850 MHz spectrometer. Only typical ligand regions are presented.

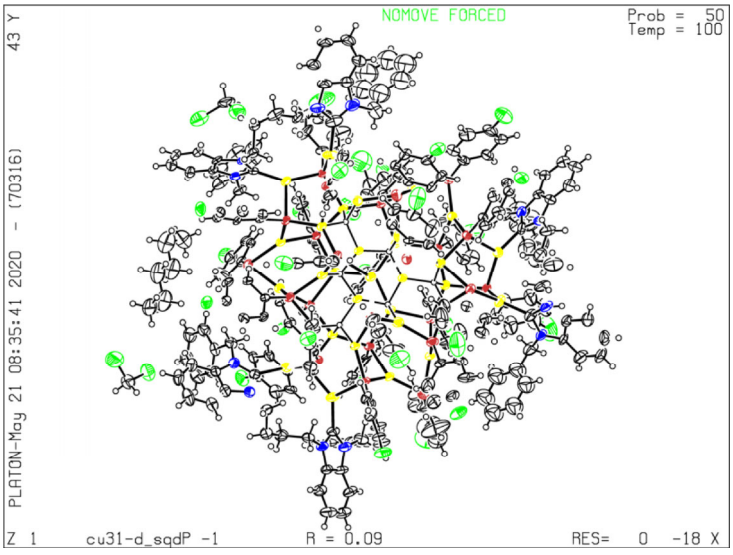

Figure S20 The thermal ellipsoids of the ORTEP diagram.

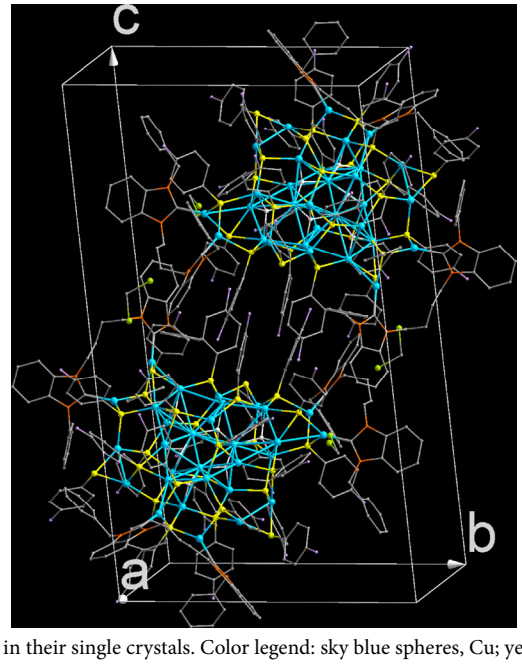

Figure S21 The packing structure of $Cu_{31}H_6$ in their single crystals. Color legend: sky blue spheres, Cu; yellow spheres, S; turquoise spheres, Cl; lavender spheres, F; orange spheres, N; gray spheres, C. Hydrogen atoms on ligands are omitted for clarity.

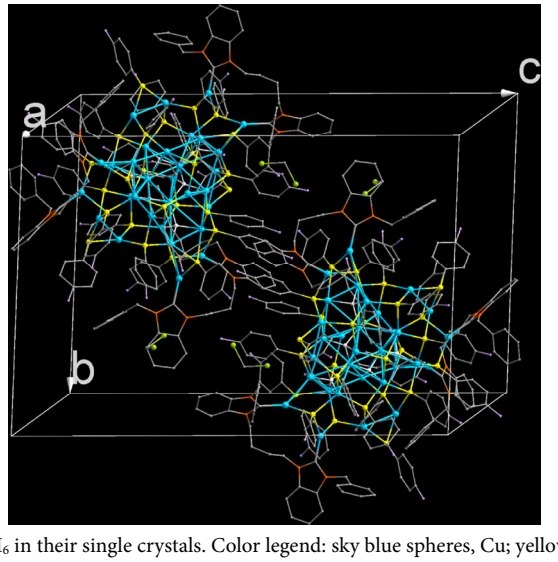

Figure S22 The packing structure of $Cu_{31}H_6$ in their single crystals. Color legend: sky blue spheres, Cu; yellow spheres, S; turquoise spheres, Cl; lavender spheres, F; orange spheres, N; gray spheres, C. Hydrogen atoms on ligands are omitted for clarity.

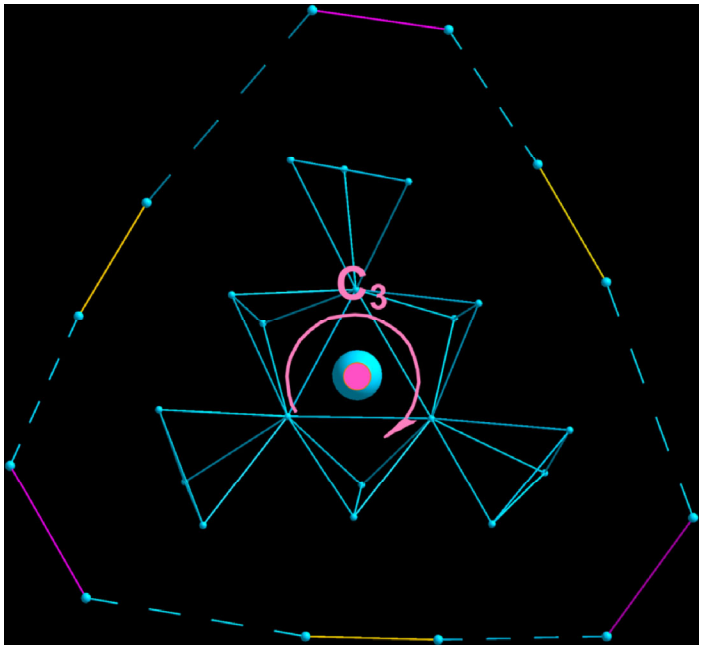

Figure S23 Metal framework of Cu_{31} in the top view of C3 symmetry axis.

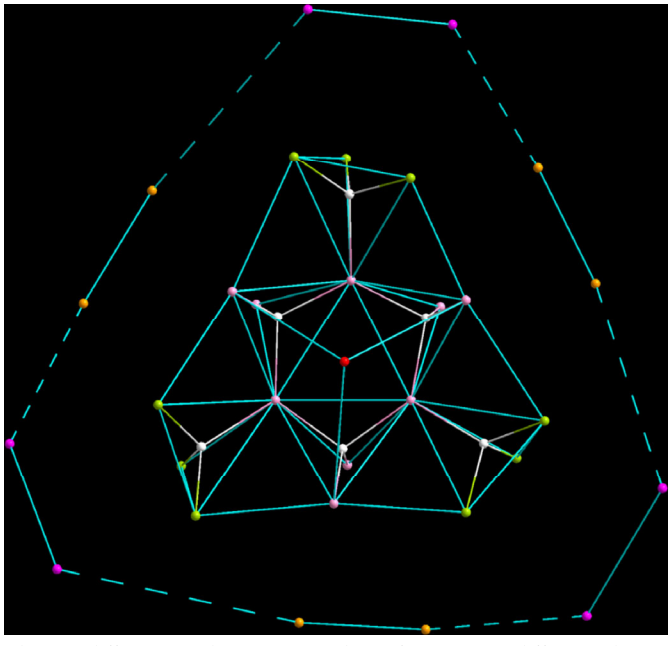

Figure S24 Metal framework of Cu_{31} showing different coordination atmosphere of Cu atoms in different colors.

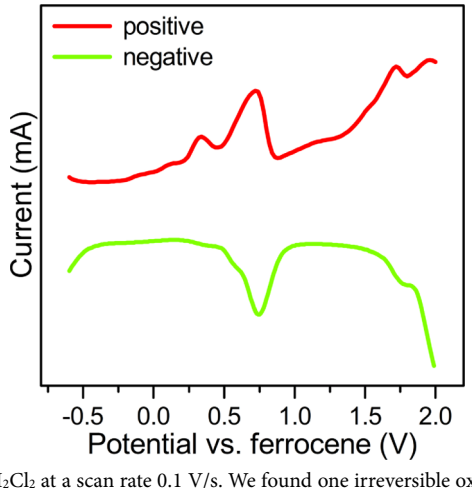

Figure S25 DPVs of Cu_{31} in 0.1 M $TBAPF_6/CH_2Cl_2$ at a scan rate 0.1 V/s. We found one irreversible oxidation at potential 0.33 V (vs. Fc/Fc^+), two quasi reversible oxidations at E1/2 = 0.73 V and 1.72 V.

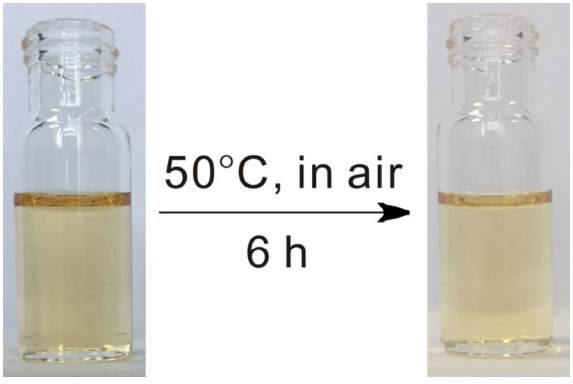

Figure S26 Photographs of $Cu_{31}H_6$ clusters before and after thermal treatment at 50 °C in 1,2-dichloroethane for 6 h under air atmosphere, showing the its ultrastability.

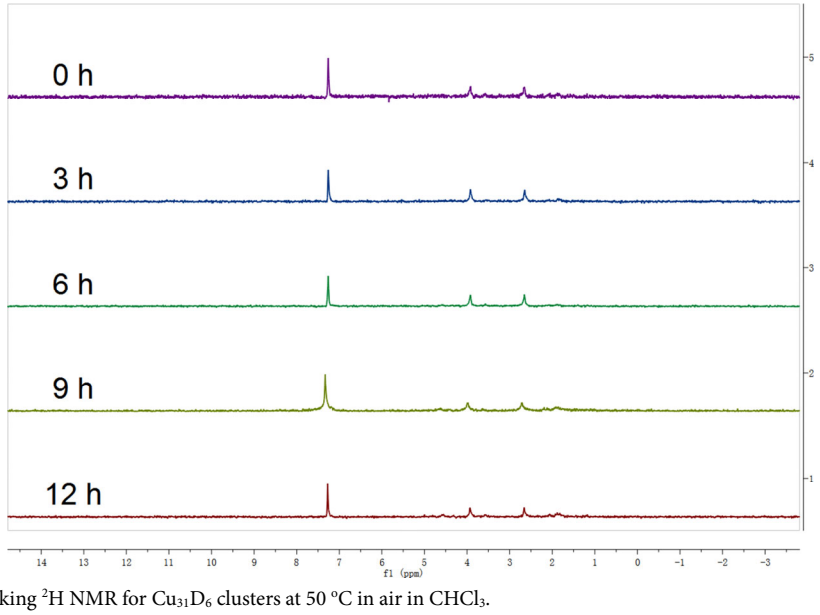

Figure S27 More-time tracking ^2H NMR for $Cu_{31}D_6$ clusters at 50 °C in air in $CHCl_3$.

Table S1 Crystal data and structure refinement for $Cu_{31}(RS)_{25}(NHC)_3H_6$.

Identification code	$Cu_{31}(RS)_{25}(NHC)_3H_6$
Empirical formula	$C_{255}H_{216}Cl_6Cu_{31}F_{25}N_{12}S_{25}$
Formula weight	6907.33
Temperature/K	100.00(10)
Crystal system	triclinic
Space group	P-1
a/Å	19.6020(3)
b/Å	22.4360(3)
c/Å	34.2772(5)
α/°	86.2820(10)
β/°	79.7030(10)
γ/°	65.9720(10)
Volume/Å^3	13546.2(4)
Z	2
ρ_{calc}g/cm^3	1.693
μ/mm^{-1}	5.446
F(000)	6912.0
Crystal size/mm^3	0.2 × 0.2 × 0.1
Radiation	CuK\a (λ = 1.54184)
2Θ range for data collection/°	3.380 to 61.168

Index ranges	$-22 \le h \le 22, -25 \le k \le 24, -38 \le l \le 38$
Reflections collected	41562
Independent reflections	30635 [R_{int} = 0.0889, R_{sigma} = 0.0968]
Data/restraints/parameters	30635/326/3152
Goodness-of-fit on F^2	1.084
Final R indexes [I>=2σ (I)]	R_1 = 0.0862, wR_2 = 0.2292
Final R indexes [all data]	R_1 = 0.1129, wR_2 = 0.2517
Largest diff. peak/hole / e $Å^{-3}$	1.87/ -1.53

Table S2 A summary of the average Cu-X (X=Cu, H, S, C) distances in the $Cu_{31}(RS)_{25}(NHC)_3H_6$ (color mark see Figure S23).

Bonds	Average Distance (Å)	Bonds	Average Distance (Å)
Cu_{rose}-Cu_{rose}	2.835	Cu_{rose}-Cu_{red}	3.203
Cu_{rose}-Cu_{lime}	2.925	Cu_{lime}-Cu_{lime}	2.770
Cu_{pink}-Cu_{pink}	3.265	Cu_{orange}-Cu_{orange}	2.642
Cu_{rose}-H	1.757	Cu_{lime}-H	1.755
Cu-S	2.286	Cu-C	1.910

References

[1] Liu, X.; Yu, G.; Li, J.; Wang, D.; Chen, Y.; Shi, K.; Chen, B., *Synlett* **2013,** *24,* 1588-1594.
[2] Penney, A. A.; Sizov, V. V.; Grachova, E. V.; Krupenya, D. V.; Gurzhiy, V. V.; Starova, G. L.; Tunik, S. P., *Inorg. Chem.* **2016,** *55,* 4720-4732.
[3] N. I. Korotkikh; V. S. Saberov; A. V. Kiselev; N. V. Glinyanaya; K. A. Marichev; T. M. Pekhtereva; G. V. Dudarenko; N. A. Bumagin; Shvaika, O. P., *Chem. Heterocyclic Com.* **2012,** *47,* 1551-1560.
[4] Ghosh, A.; Huang, R.-W.; Alamer, B.; Abou-Hamad, E.; Hedhili, M. N.; Mohammed, O. F.; Bakr, O. M., *ACS Materials Lett.* **2019,** *1,* 297-302.
[5] Chen, A.; Kang, X.; Jin, S.; Du, W.; Wang, S.; Zhu, M., *J. Phys. Chem. Lett.* **2019,** *10,* 6124-6128.
[6] CrysAlisPro Version 1.171.35.19. (2011). *Agilent Technologies Inc. Santa Clara,* CA,USA.
[7] Sheldrick, G. M. *Acta Cryst. A* **2015,** *71,* 3.
[8] Sheldrick, G. M. *Acta Cryst. A* **2008,** *64,* 112.
[9] Dolomanov, O. V.; Bourhis, L. J.; Gildea, R. J.; Howard, J. A. K.; Puschmann, H. *J. Appl. Cryst.* **2009,** *42,* 339.
[10] Huebschle, C. B.; Sheldrick, G. M.; Dittrich, B. *J. Appl. Cryst.* **2011,** *44,* 1281.
[11] Enkovaara, J.; Rostgaard, C.; Mortensen, J. J.; Chen, J.; Dulak, M.; Ferrighi, L.; Gavnholt, J.; Glinsvad, C.; Haikola, V.; Hansen, H. A.; Kristoffersen, H. H.; Kuisma, M.; Larsen, A. H.; Lehtovaara, L.; Ljungberg, M.; Lopez-Acevedo, O.; Moses, P. G.; Ojanen, J.; Olsen, T.; Petzold, V.; Romero, N. A.; Stausholm-Moller, J.; Strange, M.; Tritsaris, G. A.; Vanin, M.; Walter, M.; Hammer, B.; Hakkinen, H.; Madsen, G. K.; Nieminen, R. M.; Norskov, J. K.; Puska, M.; Rantala, T. T.; Schiotz, J.; Thygesen, K. S.; Jacobsen, K. W., *J Phys Condens Matter* **2010,** *22,* 253202.
[12] Perdew, J. P.; Burke, K.; Ernzerhof, M., *Phys. Rev. Lett.* **1996,** *77,* 3865-3868.
[13] Bader, R. F. W., Oxford University Press: New York, 1990.
[14] Tang, W.; Sanville, E.; Henkelman, G., *J. Phys. Condens. Matter.* **2009,** *21,* 084204.
[15] Walter, M.; Hakkinen, H.; Lehtovaara, L.; Puska, M.; Enkovaara, J.; Rostgaard, C.; Mortensen, J. J., *J. Chem. Phys.* **2008,** *128,* 244101-244110.
[16] Walter, M.; Akola, J.; Lopez-Acevedo, O.; Jadzinsky, P. D.; Calero, G.; Ackerson, C. J.; Whetten, R. L.; Grönbeck, H.; Häkkinen, H., *Proc. Natl. Acad. Sci.* **2008,** *105,* 9157-9162.
[17] Koster, A.; Geudtner, G.; Alvarez-Ibarra, A.; Calaminici, P.; Casida, M.; Carmona- Espindola, J.; Dominguez, V.; Flores-Moreno, R.; Gamboa, G.; Goursot, A. e. a., deMon2k, Version 6, The deMon developers, Cinvestav, Mexico City 2018, http: //www.demon-software.com/.
[18] Pritchard, B. P.; Altarawy, D.; Didier, B.; Gibson, T. D.; Windus, T. L., *J. Chem. Inf. Model.* **2019,** *59,* 4814-4820.
[19] Calaminici, P.; Janetzko, F.; Köster, A. M.; Mejia-Olvera, R.; Zuniga-Gutierrez, B., *J. Chem. Phys.* **2007,** *126,* 044108.